Journal of Biological Physics (2023) 49:345–361
https://doi.org/10.1007/s10867-023-09635-1

RESEARCH

In-phase and anti-phase bursting dynamics and synchronisation scenario in neural network by varying coupling phase

Thazhathethil Remi[1] · **Pallimanhiyil Abdulraheem Subha**[1]

Received: 3 January 2023 / Accepted: 29 March 2023 / Published online: 17 May 2023

Abstract
We have analysed the synchronisation scenario and the rich spatiotemporal patterns in the network of Hindmarsh-Rose neurons under the influence of self, mixed and cross coupling of state variables which are realised by varying coupling phase. We have introduced a coupling matrix in the model to vary coupling phase. The excitatory and inhibitory couplings in the membrane potential induce in-phase and anti-phase bursting dynamics, respectively, in the two coupled system. When the off-diagonal elements of the matrix are zero, the system shows self coupling of the three variables, which helps to attain synchrony. The off-diagonal elements give cross interactions between the variables, which reduces synchrony. The stability of the synchrony attained is analysed using Lyapunov function approach. In our study, we found that self coupling in three variables is sufficient to induce chimera states in non-local coupling. The strength of incoherence and discontinuity measure validates the existence of chimera and multichimera states. The inhibitor self coupling in local interaction induces interesting patterns like Mixed Oscillatory State and clusters. The results may help in understanding the spatiotemporal communications of the brain, within the limitations of the size of the network analysed in this study.

Keywords Cross coupling · Stability analysis · Travelling chimera · Synchronicity

PACS 05.45.-a · 05.45.Xt

1 Introduction

The mechanism of synapses in both synchronised and desnchronised neural oscillations has gained attraction due to its vital role in the propagation and exchange of information between neurons [1–3]. The synapses are broadly classified as electrical and chemical. At

✉ Pallimanhiyil Abdulraheem Subha
pasubha@farookcollege.ac.in

Thazhathethil Remi
remi@farookcollege.ac.in

[1] Department of Physics, Farook College University of Calicut, Kerala, India 673632

electrical synapses, the neurons are connected through a gap junction and a direct flow of electrical currents occurs. Hence, electrical synapses are much faster than chemical synapses [4]. Electrical synapses have great contributions to neural functions at the initial stage and continue to function throughout life by controlling sensory processing, rhythmic behaviour, pattern generation and motor systems [5].

Earlier, it was assumed that electrical synapses could induce in-phase synchrony only. But, later it was proved wrong [3] and stable anti-phase oscillations in electrically coupled relaxation oscillators were reported [6]. The stochastic transitions between in-phase and anti-phase synchronisations in neural oscillators are still of great interest even after these many years [7, 8]. Researchers have proposed different modifications in inhibitory and excitatory connections to induce anti- and in-phase oscillations [9, 10]. Memristor effects were also used for this purpose [11]. The anti- and in-phase relay synchronisation of oscillators were found in a heterogeneous network of two-dimensional lattices of continuous-time systems [8].

The study of synchronisation in networks of coupled nonlinear oscillators is an active area of research. The interplay of noise, time delay, and topology was analysed in a coupled network to understand the formation of coherence [12]. Studies have found synchronisation in weakly coupled systems, indicating that strong coupling is not always a prerequisite for synchrony [13]. Surprisingly, studies have shown that seemingly adverse factors, such as time delay and noise, can induce synchronisation in a network of coupled oscillators [14, 15].

The synchronisation of neural networks in numerous brain regions, including the hippocampus, thalamus, neocortex and cerebellar cortex, is characterised by the transition between anti-phase and in-phase oscillations in neurons [16]. When the coupled neurons fire at the same time, then it is called in-phase oscillations. Anti-phase oscillations arise when one neuron exhibits spiking behaviour while the other neuron is in rest [17]. The long range in-phase oscillations are considered to be beneficial for the coordination of various functions taking part in different parts of the brain [18]. These rhythmic transitions are also crucial for animal mobility [9]. Anti-phase oscillations were observed experimentally in different functions such as attention task, sleeping and resting state of the neurons [19–24]. A model consisting of two electrically coupled pacemakers was analysed to study the in-phase and anti-phase oscillations [25]. The factors that lead to stable anti-phase were analysed in the model of neurons with biological applications [26, 27]. Travelling chimera were used to identify the tumorous cells [28].

A chimera state is a peculiar state where a network of identical oscillators splits into two groups, one of which oscillates in synchrony while the other is incoherent. Wolfrum and Omel'chenko showed that chimera states can be observed in finite-sized systems, which is a significant finding because previously these states were only observed in systems with a thermodynamic limit [29]. The importance of chimera states and travelling waves were clinically studied and the results were numerically confirmed using FHN and leaky integrate-and-fire model [30]. Interesting spatio temporal patterns like chimeras, mutichimeras, alternating chimeras and travelling chimeras are of special interest to the researchers [31–34]. A novel type of chimera called switching chimera which attracts initial conditions and exhibits power-law switching behaviour in networks of coupled oscillators is reported [35]. Cluster formations are considered to be the intermediate stage before attaining complete synchrony [36]. Chimeras can be induced in a network by distance dependent coupling [37, 38], non-local coupling [39], cross coupling or rotation matrix coupling [40], modifications in initial conditions and topology [41] or just as an inherent property where the incoherent subpopulation stabilises the coherent subpopulation [42]. Whatever may be the mechanism behind the chimera state, the underlying principle is symmetry breaking [43]. Metastable chimeras were

obtained in Kuramoto oscillators by giving a phase lag between the different oscillators [44]. The generation of interesting phenomena such as phase synchronisation, chimera states, and travelling waves was explained in Kuramoto oscillators using this phase lag between oscillators [45]. The cross coupling of state variables was realised with the help of a rotation matrix by Omelchenko et al. to introduce multichimera states in non-locally coupled FitzHugh-Nagumo (FHN) oscillators [46]. The analysis of the rotation matrix on FHN was elaborated by other researchers [30, 47] and was also carried out on second order Hindmarsh-Rose(HR) neurons [40], by fixing the coupling phase. The authors have carried out an experimental analysis on electronic neurons and reported that in-phase synchrony happens for positive couplings and anti-phase oscillations for negative couplings in electrical coupling. Whereas, in the chemical coupling, excitatory mode produces in-phase synchrony and anti-phase oscillations result from inhibitory mode [48]. The interesting phenomena of producing in-phase and anti-phase oscillations for moderate and strong coupling in the electrical synapse in Hindmarsh-Rose neurons is also studied [49]. In this work, coupling phase is used to switch between in-phase and anti-phase bursting.

The researchers rely on the master stability function or Lyapunov function approach to analyse the stability attained by the network [50–55]. The Lyapunov function is also used as a controller to induce clusterisation in a network [36]. The Hindmarsh-Rose neurons have been widely used in computational neuroscience to study the dynamics of neural activity [56] and has contributed to our understanding of the brain and how it works [38, 57–59].

We analyse the synchronisation scenario and pattern formations in HR neural network coupled by a rotation matrix which helps to realise different coupling schemes such as self, cross and mixed modes, by varying the coupling phase. The work is organised as follows: The model for two coupled HR systems and the generation of in-phase and anti-phase oscillations are presented in Sect. 2. The synchronisation scenario and the analysis of its stability using the Lyapunov function approach have also been discussed in this section. Section 3 has been devoted to the analysis of N coupled network with self and cross coupling of variables. The synchrony of the network is quantified and the patterns obtained are presented. The quantifiers for incoherence, chimera, multichimera and coherence have also been calculated. Section 4 concludes the study.

2 A system of two coupled Hindmarsh-Rose neurons

A system of two coupled HR neurons have been analysed under the influence of self, mixed and cross coupling of state variables [28, 40]. The dynamic system is expressed by the equations of the form:

$$\begin{aligned}
\dot{x_i} &= y_i - ax_i^3 + bx_i^2 - z_i + I + g[b_{11}(x_j - x_i) + b_{12}(y_j \\
&\quad - y_i) + b_{13}(z_j - z_i)], \\
\dot{y_i} &= c - dx_i^2 - y_i + g[b_{21}(x_j - x_i) + b_{22}(y_j - y_i) + b_{23} \\
&\quad (z_j - z_i)], \\
\dot{z_i} &= r(s(x_i - x_e) - z_i) + g[b_{31}(x_j - x_i) + b_{32}(y_j - y_i) \\
&\quad + b_{33}(z_j - z_i)], i, j = 1, 2.
\end{aligned} \tag{1}$$

The membrane potential of the neuron is represented by x_i. The flow of Na^+ ions constitute the spiking variable, y_i, whereas, the bursting variable z_i is constituted by the

flow of Ca^+ ions [60]. The activation and inactivation of the fast and slow ion channels are denoted by the parameters a, b, R and x_e, respectively [56, 61]. Constants r and s approximate the biological behaviour of the model [62]. g represents the coupling strength and I is the external current entering the neuron. The interaction takes place through a cross coupling scheme between the variables x_i, y_i and z_i, which is modelled through a coupling matrix as,

$$B = \begin{pmatrix} b_{11} & b_{12} & b_{13} \\ b_{21} & b_{22} & b_{23} \\ b_{31} & b_{32} & b_{33} \end{pmatrix}$$

The system is analysed under the influence of the rotational matrix of the form:

$$B = \begin{pmatrix} \cos\delta & \sin\delta & 0 \\ -\sin\delta & \cos\delta & 0 \\ 0 & 0 & 0 \end{pmatrix} \tag{2}$$

where δ, within the interval $[-\pi,\pi)$, is the coupling phase. The different values of δ give the coupling matrices that enable us to realise self, mixed and cross couplings, in inhibitory and excitatory modes. For eg. when $\delta = 0$, the elements of the matrix are $b_{11} = 1, b_{12} = 0, b_{21} = 0$ and $b_{22} = 1$. These elements induce the self coupling in x and y of Eq. 1. When $\delta = \pi/2$, we have $b_{11} = 0, b_{12} = 1, b_{21} = -1$ and $b_{22} = 0$. Here the x variable is cross coupled to y and vice versa. Also, the cross coupling of x in y is inhibitory. Similarly, when $\delta = \pi/4$, we have mixed interactions between the x and y variables. Thus, the coupling phase represents how a variable is coupled to another variable of the same neuron. The coupling matrix in Eq. 2 helps to simplify the representation and realisation of these interactions by adjusting a single parameter δ. By continuously varying the value of δ, we can analyse the bifurcation point at which the effect of cross interaction overrides the effect of self coupling, and vice versa. The parameters are chosen as: $a = 1$, $b = 3$, $c = 1$, $d = 5$, $r = 0.006$, $s = 4$, $x_e = -1.61$, $I = 3.1$ [63]. Initial conditions are chosen randomly to lie in the range [−0.5,0.5]. The results presented in the entire work are consistent for any choice of initial values. The anti-phase and in-phase bursting dynamics in the system with electrical coupling in self, mixed and cross interactions in x and y variables is analysed by varying δ in Eq. 2 and the plots are shown in Fig. 1. When $\delta = -\pi$, the self coupling is inhibitor in x and y. The system shows anti-phase bursts as shown in Fig. 1a. When $\delta = -\frac{\pi}{2}$, the coupling is cross in x and y, that is, activator-inhibitor mode and the system exhibits anti-phase bursting as shown in Fig. 1b. In this case, the cross coupling of y variable to x is inhibitory. The self activator synapse in x and y is realised with $\delta = 0$ and the system shows in-phase burst synchrony as shown in Fig. 1c. When $\delta = \frac{\pi}{4}$, the coupling is mixed (self and cross), with activator self coupling and activator-inhibitor cross coupling. The oscillations of the neurons are in-phase as shown in Fig. 1d. The activator cross coupling of y variable in x, when $\delta = \frac{\pi}{2}$, induces in-phase synchrony, as shown in Fig. 1e. However, the synchrony is obtained at a comparatively high coupling strength as the coupling of x in y is inhibitory. An activator-activator cross coupling is realised when b_{21} is chosen to be positive which promotes synchronisation at a weaker coupling strength as shown in Fig. 1f. The system exhibits anti-phase oscillations for inhibitor coupling in the x variable and in-phase synchrony for activator coupling, whether the coupling is self or cross. Synchrony is obtained at a lower coupling strength when the nature of the connection is activator-activator in cross-coupling.

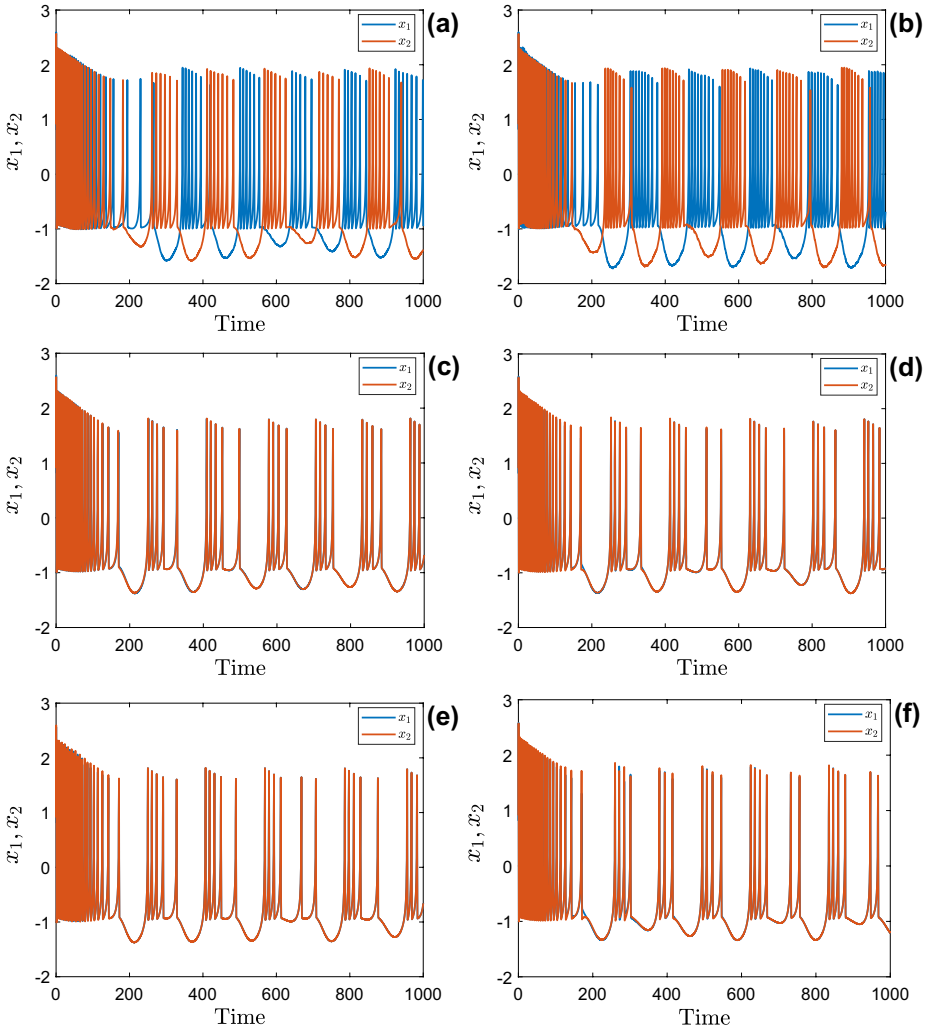

Fig. 1 Time series of membrane potential of two coupled HR neurons for different coupling phases. **a** $\delta = -\pi$, $g = 0.02$, **b** $\delta = \frac{-\pi}{2}$, $g = 0.04$, **c** $\delta = 0$, $g = 0.02$, **d** $\delta = \frac{\pi}{4}$, $g = 0.09$, **e** $\delta = \frac{\pi}{2}$, $g = 0.32$, **f** $\delta = \frac{\pi}{2}, g = 0.12, b_{21} = \sin\delta$

2.1 Synchronisation scenario

The synchrony in the system is analysed with the help of normalised synchronisation error given by the equation [64]:

$$E = \sqrt{\frac{e_x^2 + e_y^2 + e_z^2}{x_1^2 + y_1^2 + z_1^2 + x_2^2 + y_2^2 + z_2^2}} \tag{3}$$

where, $e_x = x_2 - x_1, e_y = y_2 - y_1, e_z = z_2 - z_1$. The synchronisation scenario of two coupled systems has been analysed for self coupling in x, y and z variables and is shown in Fig. 2. The blue line represents the synchronisation error with self coupling in x alone which is realised with $b_{11} = 1$ and all the other components are zero. The synchrony is obtained at $g \approx 0.5$. The self coupling in y along with x, realised with $b_{11} = b_{22} = 1$, helps to induce synchrony at a lower coupling strength. The red line shows that synchrony is obtained at $g \approx 0.01$. When $b_{11} = b_{22} = b_{33} = 1$, i.e. self coupling in x, y and z variables further reduces the value of g at which synchrony is obtained, as represented by the yellow line. The coupling strength at which synchronisation is obtained decreases as the number of self coupled variables increases.

2.1.1 Stability of synchronisation

The stability of the synchrony induced under in-phase bursting dynamics is analytically verified in this section. The coupling matrix is taken of the form as in Eq. 2. This matrix is a simple way to realise self activator coupling (b_{11},b_{22}) and activator-inhibitor cross coupling (b_{12},b_{21}) by a single parameter δ. The choice of cross coupling in and of z variable is discarded, because only cross coupling in x and y exhibits bursting dynamics. We have analysed the system of HR neurons in three different cases: (i) Self coupling in x and y, $\delta = 0$. (ii) mixed coupling in x and y, $\delta = \frac{\pi}{4}$. (iii) Cross coupling in x and y, $\delta = \frac{\pi}{2}$.

The time derivative of the Lyapunov function is used to determine the stability of the system under the influence of different coupling phases [65]. The complete synchronisation of the coupled system occurs when the two neurons exhibit identical behaviour, that is,

$$\begin{aligned} ||x_2(t) - x_1(t)|| &\to 0 \\ ||y_2(t) - y_1(t)|| &\to 0 \\ ||z_2(t) - z_1(t)|| &\to 0 \end{aligned} \tag{4}$$

For synchronised states,

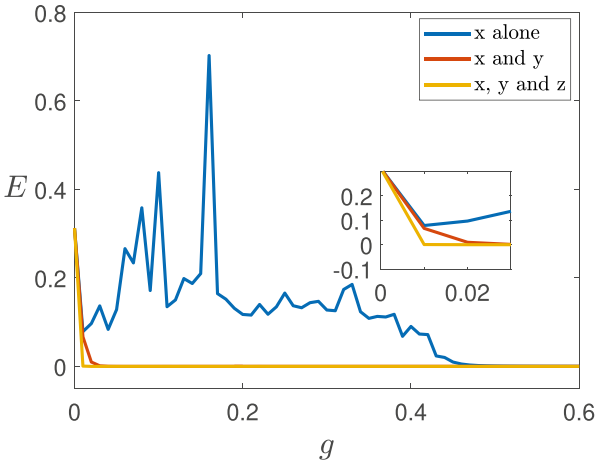

Fig. 2 Synchronisation error of two coupled HR neurons for self coupling in state variables

$$\begin{aligned} x_1(t) &= x_2(t) = x(t) \\ y_1(t) &= y_2(t) = y(t) \\ z_1(t) &= z_2(t) = z(t) \end{aligned} \tag{5}$$

The error states $e_x = x_2 - x_1, e_y = y_2 - y_1, e_z = z_2 - z_1$, are defined by introducing coordinates that are transverse to the synchronisation manifold. We have the error dynamics of the system without self coupling in z variable as:

$$\begin{aligned} \dot{e_x} &= e_y - a(x_2^3 - x_1^3) + b(x_2^2 - x_1^2) - e_z - 2g\cos\delta e_x \\ &\quad - 2g\sin\delta e_y \\ \dot{e_y} &= -d(x_2^2 - x_1^2) - e_y + 2g\sin\delta e_x - 2g\cos\delta e_y \\ \dot{e_z} &= rse_x - re_z \end{aligned} \tag{6}$$

We define a new variable $U = x_2 + x_1$. Then, $x_2^2 - x_1^2 = Ue_x$ and $x_2^3 - x_1^3 = e_x(e_x^2 + 3U^2)/4$ On simplifying,

$$\begin{aligned} \dot{e_x} &= (-0.25a(e_x^2 + 3U^2) + bU - 2g\cos\delta)e_x + (1 - 2g\sin\delta)e_y - e_z \\ \dot{e_y} &= (2g\sin\delta - dU)e_x - (1 + 2g\cos\delta)e_y \\ \dot{e_z} &= rse_x - re_z \end{aligned} \tag{7}$$

The Lyapunov functions are evaluated from this error dynamics. In Lyapunov function approach, we define a continuous, positive-definite Lyapunov function V, using Eq. 7, which has the form:

$$V(e_x, e_y, e_z) = \frac{1}{2}[e_x^2 + e_y^2 + e_z^2] \tag{8}$$

The first derivative of the Lyapunov function is continuous and the time derivative along trajectories of the error dynamical system gives

$$\frac{dV}{dt} = e_x\dot{e_x} + e_y\dot{e_y} + e_z\dot{e_z} \tag{9}$$

On substitution and simplifying,

$$\begin{aligned} \frac{dV}{dt} &= (-0.25a(e_x^2 + 3U^2) + bU - 2g\cos\delta)e_x^2 - (1 + 2g \\ &\quad \cos\delta)e_y^2 - re_z^2 + (1 - dU)e_xe_y + (rs - 1)e_xe_z \end{aligned} \tag{10}$$

The terms x_1, x_2, e_x, e_y, e_z in Eq. 10 are obtained by solving Eqs. 1 and 7 simultaneously. Similarly, the Lyapunov function for the system with self coupling in z variable is obtained as:

$$\begin{aligned} \frac{dV}{dt} &= (-0.25a(e_x^2 + 3U^2) + bU - 2g\cos\delta)e_x^2 - (1 + 2g \\ &\quad \cos\delta)e_y^2 - (r + 2g)e_z^2 + (1 - dU)e_xe_y + (rs - 1)e_xe_z \end{aligned} \tag{11}$$

The stability of the synchrony in the system by varying coupling phases given in Eq. 2 is analysed with $b_{33} = 0$ and $b_{33} = 1$ using Eqs. 10 and 11, respectively. The variations in $\frac{dV}{dt}$ with g and $b_{33} = 0$ is presented in Fig. 3a. The value of $\frac{dV}{dt}$ is greater than 0 for $g < 0.06$, in the system with self coupling in x and y ($\delta = 0$), represented by the blue line. The system exhibits desynchrony in this region. For $g > 0.06$, the system is synchronised with $\frac{dV}{dt} = 0$. For the system with mixed coupling ($\delta = \frac{\pi}{4}$), the synchrony is obtained at a higher value of $g = 0.12$, represented by the red line. The complete synchrony in the system with cross coupling ($\delta = \frac{\pi}{2}$) is obtained at $g = 0.2$. The inset shows that synchrony is more difficult to achieve in systems with mixed coupling than in systems with self coupling. The variation in $\frac{dV}{dt}$ for the system with self coupling in z variable ($b_{33} = 1$) along with cross coupling in x and y is analysed using eq. (11) and is presented in Fig. 3b. In contrast to a system lacking self coupling in z, synchrony stabilisation occurs at lower values of g. The synchrony is attained at $g = 0.02, 0.03, 0.07$ for self, mixed and cross coupling, respectively. In the inset, it is justified that in mixed coupled systems the coupling strength at which synchrony is obtained is greater than self coupled systems. When $\delta = \frac{\pi}{2}$, the interaction is cross alone and the synchrony is obtained at high coupling strength compared to the system with self and mixed coupling.

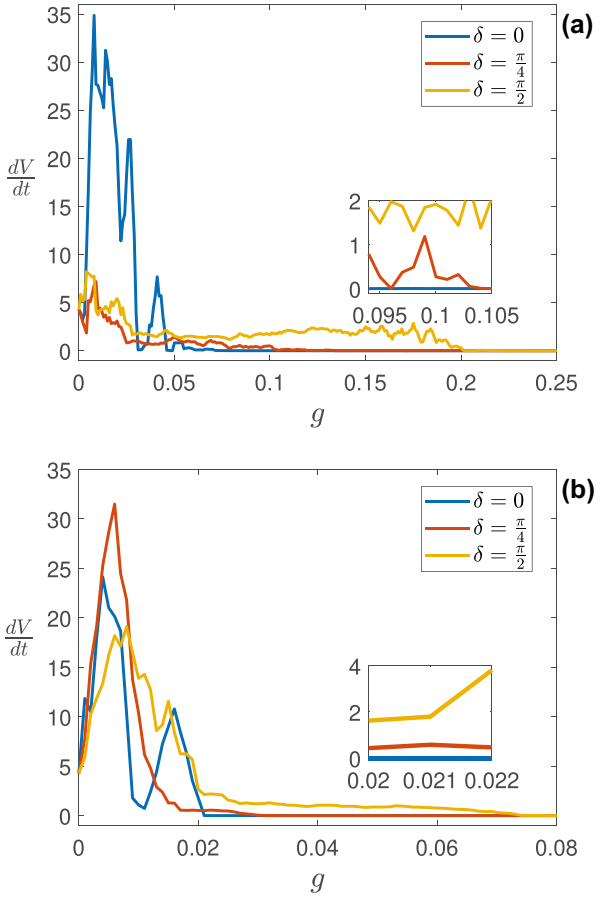

Fig. 3 Variations in derivative of Lyapunov function with coupling strength, for different values of δ. **a** $b_{33} = 0$, **b** $b_{33} = 1$

The system with self coupling attains synchrony at low coupling strength compared to a system with sole cross coupling. Cross coupling has a desynchronising impact while self coupling has a synchronising effect.

The parameter space shown in Fig. 4 characterises the complete synchronisation scenario by varying g and δ, for $b_{33} = 0$ and $b_{33} = 1$, at low and high coupling strength. The variations in the time derivative of the Lyapunov function with $b_{33} = 0$ is presented in Fig. 4a with low g and Fig. 4b with high g. For values near $\delta = 0$, the system has self interactions and synchrony is obtained at $g \approx 0.05$, which is visible from Fig. 4a. With the increase in the value of δ, the coupling strength at which the stabilised synchrony is obtained increases due to the contributions from cross coupling. On further increase in the value of δ, the interaction from self coupling decreases and cross coupling increases and the synchrony is obtained at a higher value of g. When $\delta = \frac{\pi}{2}$, the interaction is cross coupling alone and the synchrony is obtained at $g \approx 0.2$, which is observed from Fig. 4b.

The synchronisation scenario of the system with $b_{33} = 1$ as shown in Fig. 4c and d. For low values of δ, the interaction is self coupling and the synchrony is obtained at $g \approx 0.02$, as shown in Fig. 4c. With the increase in δ, cross coupling works along with self coupling and the value at which synchrony is obtained increases to $g \approx 0.03$. With further increase in δ, interactions are solely from cross coupling and the value of g at which synchrony obtained increases, as visible from Fig. 4d. The system with self coupling has the lowest coupling strength at which synchrony is obtained. The parameter space is rich and complex due to the coupling scheme of the network, and it remains consistent for any values of initial conditions.

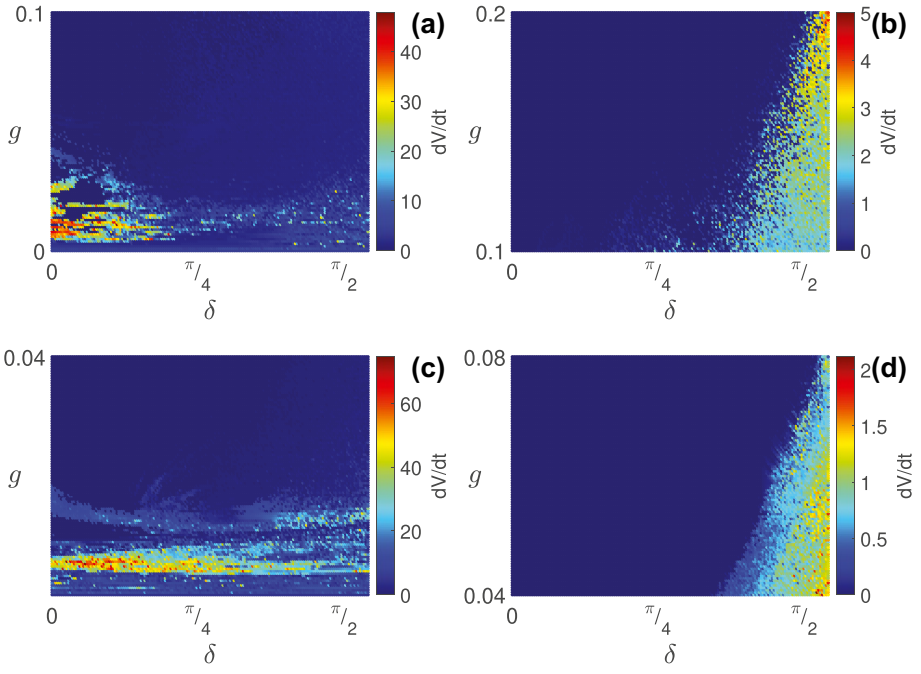

Fig. 4 Colour coded variations in time derivative of Lyapunov function with coupling strength and phase. Coupling phase is plotted along X-axis, coupling strength along Y-axis and derivative of Lyapunov function is represented by colourbar. **a** $b_{33} = 0$ (low coupling strength), **b** $b_{33} = 0$ (high coupling strength), **c** $b_{33} = 1$ (low coupling strength), **d** $b_{33} = 1$ (high coupling strength)

3 System of *N* coupled Hindmarsh-Rose neurons

A network of HR neurons with interactions represented by a rotation matrix, with global, non local and local (nearest neighbour) interactions have been analysed in a ring topology.

The dynamical equations are of the form:

$$\begin{aligned}
\dot{x}_i &= y_i + ax_i^2 - bx_i^3 - z_i + I + \frac{g}{2p}\sum_{j=i-p}^{j=i+p}[b_{11}(x_j - x_i) + \\
&\quad b_{12}(y_j - y_i) + b_{13}(z_j - z_i)], \\
\dot{y}_i &= c - dx_i^2 - y_i + \frac{g}{2p}\sum_{j=i-p}^{j=i+p}[b_{21}(x_j - x_i) + b_{22}(y_j - y_i) \\
&\quad + b_{23}(z_j - z_i)], \\
\dot{z}_i &= r(s(x_i - x_e) - z_i) + \frac{g}{2p}\sum_{j=i-p}^{j=i+p}[b_{31}(x_j - x_i) + b_{32} \\
&\quad (y_j - y_i) + b_{33}(z_j - z_i)], i = 1, 2, ..., N.
\end{aligned} \tag{12}$$

where N is the total number of neurons in the network. A periodic boundary condition $x_0 = x_N$, $x_{-1} = x_{N-1}$ and $x_{N+1} = x_1$ is considered to realise the ring configuration. p is the number of neighbours to which each neuron is coupled in either direction of the ring. The network is analysed with $N = 525$. The global, non local and local interactions are realised by fixing $p = \frac{N-1}{2}$, 10 and 1, respectively. The synchrony pattern in the network with global interaction for different coupling phases are quantified using the statistical factor of synchronisation, R [66],:

$$R = \frac{\langle F^2 \rangle - \langle F \rangle^2}{\frac{1}{N}\sum_{i=1}^{N}[\langle x_i^2 \rangle - \langle x_i \rangle^2]} \tag{13}$$

where, $F = \frac{1}{N}\sum_{i=1}^{N} x_i$ and $\langle\ \rangle$ represents the average of the variable over time. The system attains complete synchrony when $R = 1$ and desynchrony when $R = 0$.

The variations in R with g, for different values of coupling phases are shown in Fig. 5. The synchrony in the network with self coupling is presented in Fig. 5a. The synchrony attained in the system with self coupling in x variable alone is presented by the blue line. The red and yellow lines represent the synchrony pattern with self coupling in x, y and x, y, z variables, respectively. With the increase in the number of variables having self coupling, the coupling strength at which synchrony is obtained decreases. The synchrony obtained in the system with cross coupling in x and y variables and no self coupling in z variables ($b_{33} = 0$) is shown in Fig. 5b. For $g \approx 0.4$, the system attains complete synchrony for mixed coupling ($\delta = \frac{\pi}{4}$), whereas for cross coupling the complete synchrony is obtained for $g \approx 0.7$. For values above 0.7, the synchrony for mixed and cross coupling coincides with each other. The amount of synchrony obtained with cross coupling in x and y variables and self coupling in z variable ($b_{33} = 1$) is shown in Fig. 5c. In comparison to the system with no self coupling in the z variable, the synchronisation is reached at a lower coupling strength. The system attains complete synchrony at $g = 0.1$ and 0.7 for mixed and cross coupling, respectively. The coupling strength at which synchrony is achieved for N coupled neurons, however, is higher than in a system with two neurons.

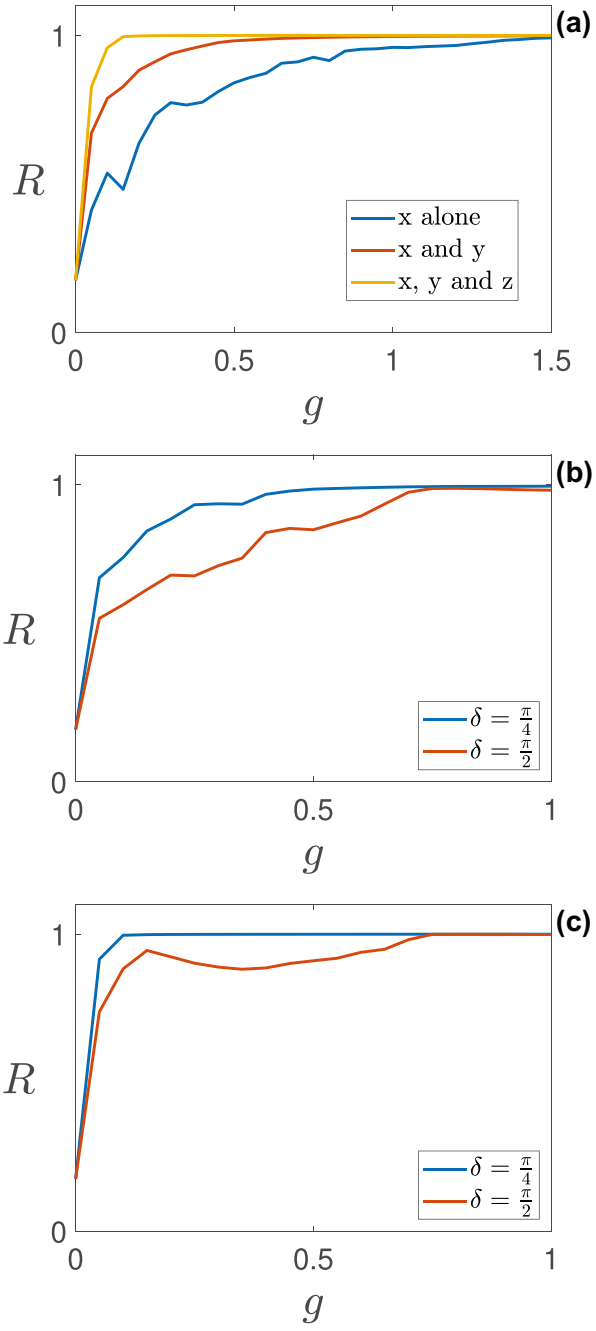

Fig. 5 The variations in Statistical factor of synchronisation with coupling strength in HR neural network with global interaction for different values of coupling phase. **a** Self coupling in variables, **b** $b_{33} = 0$, **c** $b_{33} = 1$

The network with $b_{33} = 1$ shows a richer pattern and cluster formations in non local and local interactions and is shown in Fig. 6. The multichimera pattern obtained for non local interaction in the system with self coupling in x, y and z variables, for $\delta = 0$, is shown in Fig. 6a. The self coupling in the state variables is capable of inducing

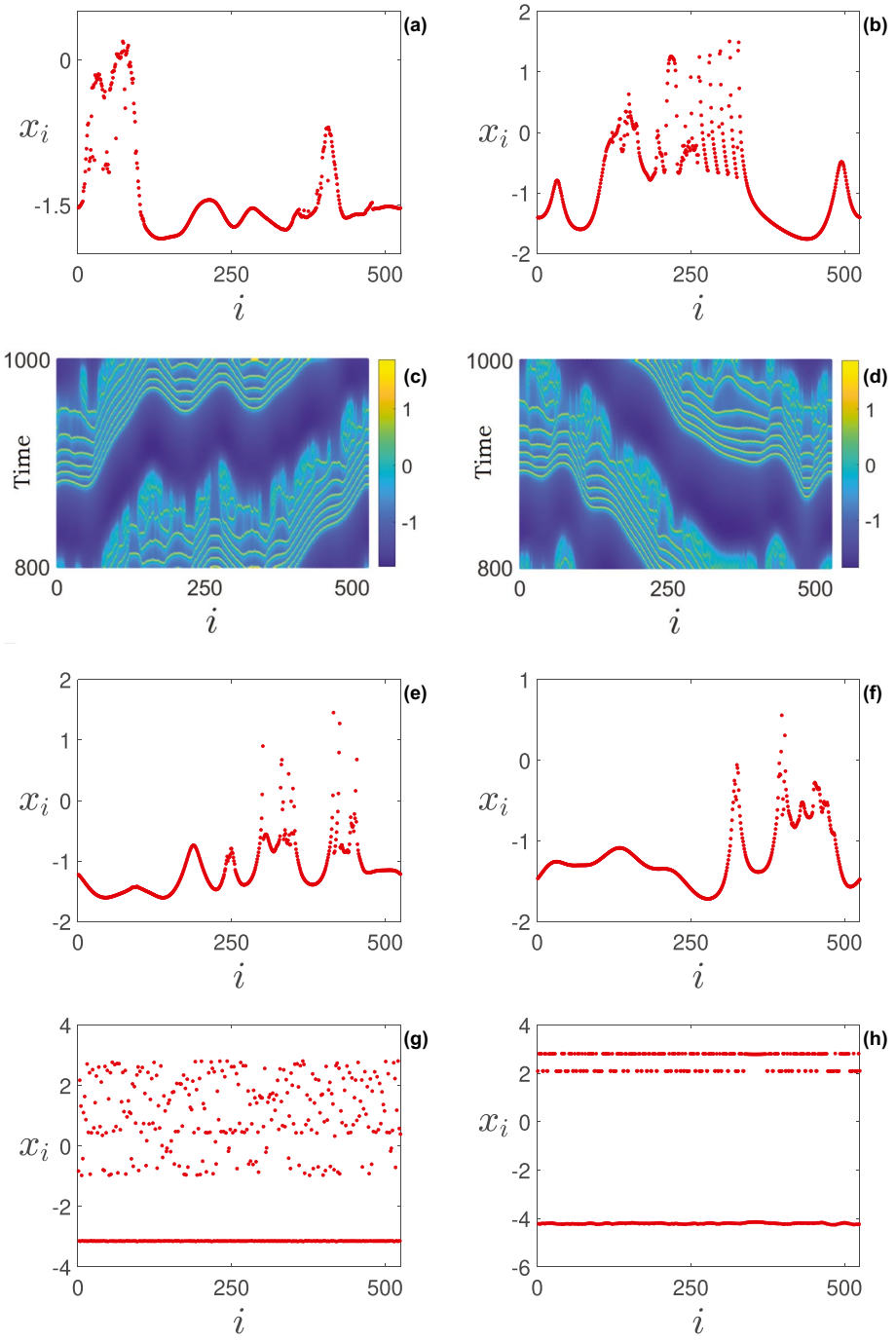

Fig. 6 Emergence of interesting patterns in HR network by the variations in coupling phase non local and local interactions. **a** multichimera ($p = 10$, $\delta = 0$, $g = 0.1$) **b** chimera ($p = 10$, $\delta = \frac{\pi}{4}$, $g = 0.19$) **c** travelling chimera ($p = 10$, $\delta = \frac{\pi}{2} - 1$, $g = 0.09$) **d** travelling chimera ($p = 10$, $\delta = \frac{\pi}{2} - 1$, $g = 0.1$) **e** multichimera ($p = 10$, $\delta = \frac{\pi}{2}$, $g = 0.17$) **f** multichimera ($p = 10$, $\delta = \frac{\pi}{2}$, $g = 0.24$) **g** MOS ($p = 1$, $\delta = -\pi$, $g = 0.2$) **h** cluster ($p = 1$, $\delta = -\pi$, $g = 0.3$)

chimera states. The same is not obtained when the coupling is in a single variable (not shown in this work). This proves that a network is self sufficient of exhibiting chimeras without distance dependent coupling or cross coupling. The mixed coupling in x and y variables and self coupling in z variable, for $\delta = \frac{\pi}{4}$ induces a chimera state as shown in Fig. 6b. Travelling chimera is obtained for mixed coupling with $\delta = \frac{\pi}{2} - 1$ for $g = 0.09$ and 0.1, as shown in Fig. 6c and d, respectively. Multichimera states are obtained for $\delta = \frac{\pi}{2}$, at $g = 0.17, 0.24$, as shown in Fig. 6e and f, respectively. The inhibitor self coupling with $\delta = -\pi$ in nearest neighbour interaction induces a mixed oscillatory state, as shown in Fig. 6g. The oscillators are grouped into three clusters for locally coupled networks, with $\delta = -\pi$ as shown in Fig. 6h.

The emergence of chimera and multichimera states in the network with self, cross and mixed coupling of state variables is analysed with the help of a quantitative measure called strength of incoherence (SI). The local standard deviation, $\sigma(m)$, has been defined from the time series. We divide the total number of oscillators into 'M' bins of equal length 'n' = N/M and obtain the difference dynamical variable as $\omega_j = x_j - x_{j+1}$. Then the local standard deviation is defined as [67]:

$$\sigma(m) = \left\langle \sqrt{\frac{1}{n} \sum_{j=n(m-1)+1}^{mn} \left[\omega_j - \langle\omega\rangle\right]^2} \right\rangle_t, \tag{14}$$

where m = 1,2,...,M; $\langle\omega\rangle = \frac{1}{N}\sum_{i=1}^{N} \omega_i(t)$. $\langle ... \rangle_t$ denotes the average over time. The term SI is defined as:

$$SI = 1 - \frac{\sum_{m=1}^{M} s_m}{M}, s_m = \mathcal{H}(\delta - \sigma(m)), \tag{15}$$

where $\mathcal{H}$ is the Heaviside step function and δ is a predefined threshold. The values of SI are 1, 0 or between 1 and 0, representing incoherent, coherent and chimera or multichimera states, respectively. In order to distinguish chimera from multichimera states, we calculate discontinuity measure (DM) [67], which is defined as:

$$DM = \frac{\sum_{i=1}^{M} |s_{i+1} - s_i|}{2}, \tag{16}$$

where $s_{M+1} = s_1$. For the chimera state, DM = 1 and for the multichimera state $2 \leq \text{DM} \leq \frac{M}{2}$.

The self coupling in three variables x, y and z induces chimera states in non locally coupled network as shown in Fig. 7a. Figure 7b justifies the presence of chimera states. The emergence of chimera or multichimera states in non locally coupled networks with mixed coupling in x, y and self coupling in z is shown in Fig. 7c. The variations in DM as shown in Fig. 7d distinguish the chimera and multichimera states. The cross coupling in x and y, along with the self coupling in the z variable also induces chimera and multichimera states in the non locally coupled network which is visible from Fig. 7e. Figure 7f shows that there are no chimeras and that the patterns obtained are multichimeras. Studies have shown that under the influence of a rotation matrix, chimera states are induced in the non locally coupled networks with self, mixed and cross interaction and in locally coupled network, neurons show clusterisation. In mixed and cross coupling, the possibilities for chimera states are minimum, but it is high for self coupling.

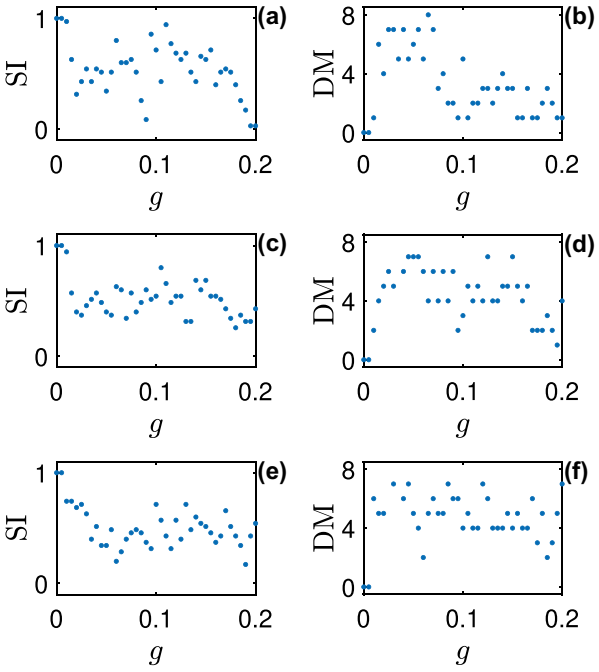

Fig. 7 Strength of incoherence (SI) and discontinuity measure (DM) for different coupling phases in non local interactions. The left panel shows the values of SI. **a** $\delta = 0$, **c** $\delta = \frac{\pi}{4}$, **e** $\delta = \frac{\pi}{2}$. The right panel shows the variations in DM for the corresponding values of left panel. Here, $M = 35$, $\delta = 0.04$, $p = 10$

4 Conclusions

The synchronisation and patterns emerging due to the self and cross interactions of variables are analysed in networks of HR neurons. Activator self coupling in the x variable induces in-phase synchrony whereas the inhibitory mode induces anti-phase synchrony in two coupled systems. When the self coupling in y and z variables are introduced synchrony is attained at a lower coupling strength. Based on the Lyapunov function approach, the stability of activator coupling in x variable is verified for self, mixed and cross coupling modes. When the system achieves synchrony, the time derivative of the function tends to zero. The synchronisation scenario is explained in detail by the parameter space with coupling phase and coupling strength, as the parameters. The complete synchronisation is achieved at a lower coupling strength when self coupling is present in the variables, and as cross interactions come into play, synchronisation is achieved at a higher coupling strength.

A network arranged in ring topology has been analysed with global, non local and local interactions. The in-phase synchrony obtained for activator coupling in x variable with self, mixed or cross coupling has been justified in the globally coupled systems as well. Chimera, multichimera and travelling chimera states are obtained by the interplay of coupling phase and coupling strength, in non local interactions. It is observed that the presence of chimera states is low, in systems with mixed or cross coupling and high in networks with self coupling. The inhibitor self coupling in x, y and activator self coupling in z variable induces in-phase, anti-phase and out of phase oscillations which result in the occurrence of mixed oscillatory state and clusters in nearest neighbour interactions.

The observed in-phase and anti-phase oscillations might be an indicator of the presence of distinct frequency rhythms and oscillatory patterns in separate regions of extended neural networks. The findings of this work reveal the dynamic processes that cause the coupled neurons to exhibit in-phase and anti-phase oscillations, which is useful for understanding how synapses regulate the rhythms of brain activity.

Acknowledgements TR would like to thank UGC, India, for the research fellowship through MANF and PAS would like to acknowledge DST, India, for the financial assistance through FIST program.

Author Contributions All authors contributed to the study conception and design. The work, data simulation and analysis were performed by T. Remi. P. A. Subha made substantial contributions to the conception or design of the work. The first draft of the manuscript was written by T. Remi and all authors commented on previous versions of the manuscript. All authors read and approved the final manuscript.

Availability of data and material The data that support the findings were generated from numerical simulations by the software MATLAB.

Code availability Code for data simulation was developed by ourselves in MATLAB and will be made available on request.

Declarations

Conflict of interest The authors declare no competing interests.

References

1. Swanson, L.W.: Brain Architecture: Understanding the Basic Plan. Oxford University Press (2012)
2. Bem, T., Le Feuvre, Y., Rinzel, J., Meyrand, P.: Electrical coupling induces bistability of rhythms in networks of inhibitory spiking neurons. Eur. J. Neurosci. **22**(10), 2661–2668 (2005)
3. Bem, T., Rinzel, J.: Short duty cycle destabilizes a half-center oscillator, but gap junctions can restabilize the anti-phase pattern. J. Neurophysiol. **91**(2), 693–703 (2004)
4. Njitacke, Z.T., Doubla, I.S., Kengne, J., Cheukem, A.: Coexistence of firing patterns and its control in two neurons coupled through an asymmetric electrical synapse. Chaos (Woodbury, NY) **30**(2), 023101 (2020)
5. Martin, E.A., Lasseigne, A.M., Miller, A.C.: Understanding the molecular and cell biological mechanisms of electrical synapse formation. Front. Neuroanat. **14**, 12 (2020)
6. Lee, E., Terman, D.: Stable antiphase oscillations in a network of electrically coupled model neurons. SIAM J. Appl. Dyn. Syst. **12**(1), 1–27 (2013)
7. Bashkirtseva, I., Ryashko, L., Pisarchik, A.N.: Stochastic transitions between in-phase and anti-phase synchronization in coupled map-based neural oscillators. Commun. Nonlinear Sci. Numer. Simul. **95**, 105611 (2021)
8. Protachevicz, P.R., Hansen, M., Iarosz, K.C., Caldas, I.L., Batista, A.M., Kurths, J.: Emergence of neuronal synchronisation in coupled brain areas. Front. Comput. Neurosci. **15**, 35 (2021)
9. Jia, B., Wu, Y., He, D., Guo, B., Xue, L.: Dynamics of transitions from anti-phase to multiple in-phase synchronizations in inhibitory coupled bursting neurons. Nonlinear Dyn. **93**(3), 1599–1618 (2018)
10. Korotkov, A.G., Kazakov, A.O., Levanova, T.A., Osipov, G.V.: The dynamics of ensemble of neuron-like elements with excitatory couplings. Commun. Nonlinear Sci. Numer. Simul. **71**, 38–49 (2019)
11. Usha, K., Subha, P.: Hindmarsh-Rose neuron model with memristors. Biosystems **178**, 1–9 (2019)
12. Masoliver, M., Malik, N., Scholl, E., Zakharova, A.: Coherence resonance in a network of FitzHugh-Nagumo systems: interplay of noise, time-delay, and topology. Chaos: An Interdisciplinary Journal of Nonlinear Science **27**(10), 101102 (2017)
13. Boaretto, B., Budzinski, R., Prado, T., Kurths, J., Lopes, S.: Neuron dynamics variability and anomalous phase synchronization of neural networks. Chaos: An Interdisciplinary Journal of Nonlinear Science **28**(10), 106304 (2018)
14. Tang, J., Ma, J., Yi, M., Xia, H., Yang, X.: Delay and diversity-induced synchronization transitions in a small-world neuronal network. Phys. Rev. E **83**(4), 046207 (2011)

15. Pakdaman, K., Mestivier, D.: Noise induced synchronization in a neuronal oscillator. Physica D **192**(1–2), 123–137 (2004)
16. Colgin, L.L.: Rhythms of the hippocampal network. Nat. Rev. Neurosci. **17**(4), 239–249 (2016)
17. Lee, E., Terman, D.: Stability of antiphase oscillations in a network of inhibitory neurons. SIAM J. Appl. Dyn. Syst. **14**(1), 448–480 (2015)
18. Vicente, R., Gollo, L.L., Mirasso, C.R., Fischer, I., Pipa, G.: Dynamical relaying can yield zero time lag neuronal synchrony despite long conduction delays. Proc. Natl. Acad. Sci. U.S.A. **105**(44), 17157–17162 (2008)
19. Lewis, C.M., Baldassarre, A., Committeri, G., Romani, G.L., Corbetta, M.: Learning sculpts the spontaneous activity of the resting human brain. Proc. Natl. Acad. Sci. U.S.A. **106**(41), 17558–17563 (2009)
20. Shmueli, K., van Gelderen, P., de Zwart, J.A., Horovitz, S.G., Fukunaga, M., Jansma, J.M., Duyn, J.H.: Low-frequency fluctuations in the cardiac rate as a source of variance in the resting-state fMRI BOLD signal. Neuroimage **38**(2), 306–320 (2007)
21. Corbetta, M., Shulman, G.L.: Control of goal-directed and stimulus driven attention in the brain. Nat. Rev. Neurosci. **3**(3), 201–215 (2002)
22. Simpson, J.R., Snyder, A.Z., Gusnard, D.A., Raichle, M.E.: Emotion induced changes in human medial prefrontal cortex: I. during cognitive task performance. Proc. Natl. Acad. Sci. U.S.A. **98**(2), 683–687 (2001)
23. Mantini, D., Perrucci, M.G., Del Gratta, C., Romani, G.L., Corbetta, M.: Electrophysiological signatures of resting state networks in the human brain. Proc. Natl. Acad. Sci. U.S.A. **104**(32), 13170–13175 (2007)
24. Horovitz, S.G., Braun, A.R., Carr, W.S., Picchioni, D., Balkin, T.J., Fukunaga, M., Duyn, J.H.: Decoupling of the brain's default mode network during deep sleep. Proc. Natl. Acad. Sci. U.S.A. **106**(27), 11376–11381 (2009)
25. Cymbalyuk, G.S., Nikolaev, E., Borisyuk, R.: In-phase and antiphase self-oscillations in a model of two electrically coupled pacemakers. Biol. Cybern. **71**, 153–160 (1994)
26. Merrison-Hort, R., Borisyuk, R.: The emergence of two anti-phase oscillatory neural populations in a computational model of the parkinsonian globus pallidus. Front. Comput. Neurosci. **7**, 173 (2013)
27. Li, D., Zhou, C.: Organization of anti-phase synchronization pattern in neural networks: what are the key factors? Front. Syst. Neurosci. **5**, 100 (2011)
28. Koulierakis, I., Verganelakis, D.A., Omelchenko, I., Zakharova, A., Scholl, E., Provata, A.: Structural anomalies in brain networks induce dynamical pacemaker effects. Chaos: An Interdisciplinary Journal of Nonlinear Science **30**(11), 113137 (2020)
29. Wolfrum, M., Omel'chenko, E.: Chimera states are chaotic transients. Phys. Rev. E **84**(1), 015204 (2011)
30. Majhi, S., Bera, B.K., Ghosh, D., Perc, M.: Chimera states in neuronal networks: A review. Phys. Life Rev. **28**, 100–121 (2019)
31. Bera, B.K., Ghosh, D., Lakshmanan, M.: Chimera states in bursting neurons. Phys. Rev. E **93**(1), 012205 (2016)
32. Simo, G.R., Louodop, P., Ghosh, D., Njougouo, T., Tchitnga, R., Cerdeira, H.A.: Traveling chimera patterns in a two-dimensional neuronal network. Phys. Lett. A **127519** (2021)
33. Dudkowski, D., Czolczynski, K., Kapitaniak, T.: Traveling chimera states for coupled pendula. Nonlinear Dyn. **95**(3), 1859–1866 (2019)
34. Majhi, S., Ghosh, D.: Alternating chimeras in networks of ephaptically coupled bursting neurons. Chaos: An Interdisciplinary Journal of Nonlinear Science **28**(8), 083113 (2018)
35. Zhang, Y., Nicolaou, Z.G., Hart, J.D., Roy, R., Motter, A.E.: Critical switching in globally attractive chimeras. Phys. Rev. X **10**(1), 011044 (2020)
36. Usha, K., Subha, P., Nayak, C.R.: The route to synchrony via drum head mode and mixed oscillatory state in star coupled Hindmarsh-Rose neural network. Chaos, Solitons Fractals **108**, 25–31 (2018)
37. Bandyopadhyay, B., Khatun, T., Dutta, P.S., Banerjee, T.: Symmetry breaking by power-law coupling. Chaos, Solitons Fractals **139**, 110289 (2020)
38. Remi, T., Subha, P., Usha, K.: Collective dynamics of neural network with distance dependent field coupling. Commun. Nonlinear Sci. Numer. Simul. **110**, 106390 (2022)
39. Zakharova, A., Kapeller, M., Scholl, E.: Chimera death: Symmetry breaking in dynamical networks. Phys. Rev. Lett. **112**(15), 154101 (2014)
40. Wang, Z., Xu, Y., Li, Y., Kapitaniak, T., Kurths, J.: Chimera states in coupled Hindmarsh-Rose neurons with α-stable noise. Chaos Solitons Fractals 148, 110976 (2021)
41. Kundu, S., Bera, B.K., Ghosh, D., Lakshmanan, M.: Chimera patterns in three-dimensional locally coupled systems. Phys. Rev. E **99**(2), 022204 (2019)
42. Zhang, Y., Motter, A.E.: Mechanism for strong chimeras. Phys. Rev. Lett. **126**(9), 094101 (2021)
43. Asllani, M., Siebert, B.A., Arenas, A., Gleeson, J.P.: Symmetry-breaking mechanism for the formation of cluster chimera patterns. Chaos: An Interdisciplinary Journal of Nonlinear Science **32**(1), 013107 (2022)
44. Shanahan, M.: Metastable chimera states in community-structured oscillator networks. Chaos: An Interdisciplinary Journal of Nonlinear Science **20**(1), 013108 (2010)

45. Budzinski, R.C., Nguyen, T.T., Joan, J., Minac, J., Sejnowski, T.J., Muller, L.E.: Geometry unites synchrony, chimeras, and waves in nonlinear oscillator networks. Chaos: An Interdisciplinary Journal of Nonlinear Science **32**(3), 031104 (2022)
46. Omelchenko, I., Omel'chenko, E., Hovel, P., Scholl, E.: When nonlocal coupling between oscillators becomes stronger: patched synchrony or multichimera states. Phys. Rev. Lett. **110**(22), 224101 (2013)
47. Wang, Z., Liu, Z.: A brief review of chimera state in empirical brain networks. Front. Physiol. **11**, 724 (2020)
48. Pinto, R.D., Varona, P., Volkovskii, A., Szucs, A., Abarbanel, H.D., Rabinovich, M.I.: Synchronous behavior of two coupled electronic neurons. Phys. Rev. E **62**(2), 2644 (2000)
49. Erichsen, R., Jr, Mainieri, M., Brunnet, L.: Periodicity and chaos in electrically coupled Hindmarsh-Rose neurons. Phys. Rev. E **74**(6), 061906 (2006)
50. Pecora, L.M., Carroll, T.L.: Master stability functions for synchronized coupled systems. Phys. Rev. Lett. **80**(10), 2109 (1998)
51. Krasovskii, N.N.: Stability of Motion. Stanford University Press (1963)
52. Parastesh, F., Azarnoush, H., Jafari, S., Hatef, B., Perc, M., Repnik, R.: Synchronizability of two neurons with switching in the coupling. Appl. Math. Comput. **350**, 217–223 (2019)
53. Hussain, I., Jafari, S., Ghosh, D., Perc, M.: Synchronization and chimeras in a network of photosensitive FitzHugh-Nagumo neurons. Nonlinear Dynamics, 1–11 (2021)
54. Zhou, P., Hu, X., Zhu, Z., Ma, J.: What is the most suitable Lyapunov function? Chaos, Solitons Fractals **150**, 111154 (2021)
55. Joshi, S.K.: Synchronization of coupled Hindmarsh-Rose neuronal dynamics: Analysis and experiments. Express Briefs, IEEE Transactions on Circuits and Systems II (2021)
56. Hindmarsh, J.L., Rose, R.: A model of neuronal bursting using three coupled first order differential equations. Proceedings of the Royal society of London. Series B. Biological sciences **221**(1222), 87-102 (1984)
57. Usha, K., Subha, P.: Star-coupled Hindmarsh-Rose neural network with chemical synapses. Int. J. Mod. Phys. C **29**(03), 1850023 (2018)
58. Usha, K., Subha, P.: Energy feedback and synchronous dynamics of Hindmarsh-Rose neuron model with memristor. Chin. Phys. B **28**(2), 020502 (2019)
59. Remi, T., Subha, P., Usha, K.: Controlling phase synchrony in the mean field coupled Hindmarsh-Rose neurons. Int. J. Mod. Phys. C **33**(05), 2250058 (2022)
60. Buric, N., Todorovic, K., Vasovic, N.: Synchronization of bursting neurons with delayed chemical synapses. Phys. Rev. E **78**(3), 036211 (2008)
61. Usha, K., Subha, P.: Collective dynamics and energy aspects of star coupled Hindmarsh-Rose neuron model with electrical, chemical and field couplings. Nonlinear Dyn. **96**(3), 2115–2124 (2019)
62. Erichsen, R., Jr, Brunnet, L.: Multistability in networks of Hindmarsh-Rose neurons. Phys. Rev. E **78**(6), 061917 (2008)
63. Shi, X., Wang, Z.: Adaptive synchronization of time delay Hindmarsh-Rose neuron system via self-feedback. Nonlinear Dyn. **69**(4), 2147–2153 (2012)
64. Buscarino, A., Frasca, M., Branciforte, M., Fortuna, L., Sprott, J.C.: Synchronization of two Rossler systems with switching coupling. Nonlinear Dyn. **88**(1), 673–683 (2017)
65. Yamakou, M.E.: Chaotic synchronization of memristive neurons: Lyapunov function versus Hamilton function. Nonlinear Dyn. **101**(1), 487–500 (2020)
66. Xu, Y., Jia, Y., Ma, J., Hayat, T., Alsaedi, A.: Collective responses in electrical activities of neurons under field coupling. Sci. Rep. **8**(1), 1–10 (2018)
67. Gopal, R., Chandrasekar, V., Venkatesan, A., Lakshmanan, M.: Observation and characterization of chimera states in coupled dynamical systems with nonlocal coupling. Phys. Rev. E **89**(5), 052914 (2014)